Environment, Development and Sustainability (2024) 26:14507–14534
https://doi.org/10.1007/s10668-023-03204-1

Causes, concerns and hazards of sinkhole formation in Brengi stream catchment of Upper Jhelum basin, Kashmir Himalaya

Riyaz Ahmad Mir[1,2] · Rayees Ahmed[2] · Majid Hussain[3] · Syed Kaiser Bukhari[3] · Pervez Ahmed[2] · Reyaz Ahmad Dar[4], et al. ***[full author details at the end of the article]***

Received: 13 July 2022 / Accepted: 26 March 2023 / Published online: 6 April 2023

Abstract

On February 11, 2022, the Brengi streambed caved in, and a sizable sinkhole (33.57 N and 75.33 E) was developed. The Brengi stream is a major tributary of the Upper Jhelum River in Kashmir Himalaya. The sinkhole swallowed the entire stream flow and caused mass mortality of fish and other aquatic creatures, besides disrupting completely the local water supplies. The present study analyzed the ancillary data reports, geological and topographic maps, satellite and Google Earth images, and climatic data in conjunction with the field, geophysical and chemical tracer studies to understand the causes of sinkhole formation, the outlet of captured flow and its associated hazards. The study indicated the sinkhole as a "Collapse Sinkhole" formed due to the collapse of the limestone (Triassic) roof cap of an existing deep-seated underground cavern through a prolonged dissolution and physical erosion by the weakly acidic stream and groundwater circulation under suitable climatic conditions. In this area, the limestone bedrock covered under a thick pile of overburden alluvial material comprises large structural discontinuities (bedding planes, fractures, joints and shear zones) and karst features. Before the collapse, a large water pool consisting ~ 80 m^3 of the water column was estimated to be at the sinkhole site. Proton Precession Magnetometer survey around the sinkhole indicated that the underlying caverns are about ~ 100 m long downstream. A stream flow of ~ 15.03 m^3/s was estimated to be swallowed by the sinkhole continuously for a couple of weeks till its closure. As a consequence, an estimated area of ~ 77.15 km^2 comprising 58% agricultural/horticultural land, 25% vegetation cover and 10% built-up area was at high risk of catastrophe downstream of the sinkhole. From the tracer study, the outlet of the sinking water was found located at 16 km downstream at Achabal springs with an average flow velocity of ~ 1.3 km/h from the sinkhole site to the outlet. The sinkhole is a part and characteristic feature of karst topography of the area. Therefore, a detailed study on sinkhole susceptibility and hazard assessment is required. Although the sinkhole formation is an event of local significance in terms of the scale of the disaster, it may be of extreme importance in planning a given investment and management of local groundwater resources and karst springs.

Keywords Brengi · Jhelum · Himalaya · Triassic Limestone · Sinkhole · Geophysical and Tracer survey · Karst Spring · Hazards

Extended author information available on the last page of the article

1 Introduction

Kashmir valley has undergone a complicated and multifaceted geological evolution and preserves significant geological events of the Himalayan orogenesis, sedimentation and volcanic activity right from Archaean times to the Recent period (GSI, 2012; Mir et al., 2016, 2023). In this part of the Himalayan region, the silicate and carbonate rocks of Paleozoic age, carbonate rocks of Triassic age, Karewa deposits of Quaternary age and Recent alluvium are the main and dominant geological units (GSI, 2012; Mir et al., 2016). The carbonate rocks are reported to cover an area of about 1100 km^2, of which 58% (631 km^2) lies toward the southern part of the Upper Jhelum basin in Kashmir valley (Jeelani et al., 2018; Shah et al., 2018). In this region, Triassic carbonate rocks are surrounded by Paleozoic rocks and are overlain by Pleistocene and Recent sediments (GSI, 2012; Mir et al., 2016; Shah et al., 2018; Jeelani et al., 2018). These Triassic carbonate rocks are well reported to provide significant karst geomorphic imprints in the form of solution features, swallow holes, sinkholes, conduits, shafts, underground and deep-seated cavers, caves and large springs. Moreover, the karst areas are reported to occur in the form of dissected ridges and are well distributed in southern areas of Kashmir valley such as Kokernag, Verinag, Achabal, Mattan, Anantnag Town, Zajibal-Sheshnag, Beerwah, Tral, Manasbal and Bandipora (Jeelani et al., 2018; Shah et al., 2018). Among, the several karst features such as caverns, conduits, shafts, karren fields and pits, the sinkholes are the most distinctive features of karst lands or karst topography and represent a direct connection in karst between the ground surface and the subterranean world (Parise, 2019). The sinkhole landforms are described as closed depressions with internal drainage and in most case a direct connection with the underground (White, 1988; Ford & Williams, 2007). The initial expression of sinkholes at the surface is typically circular in plan (Berest, 2017). In the section, a sinkhole may show different profiles as conical, cylindrical and bowl- or funnel-shaped (Parise, 2019). In terms of size, the sinkholes vary from a few meters to hundreds of meters across, with depths mostly in the range from less than 1 m to tens of meters. However, the most spectacular sinkholes may reach a depth of some hundreds of meters (Parise, 2019).

The sinkholes are among the most vulnerable sites of collapse and dangerous geohazards in karst areas and cause serious damage and losses to the infrastructure and society (Parise, 2019). The sinkhole occurrence is difficult to predict and may also be a direct and possible source of contamination of karst aquifers, karst springs, and groundwater (Parise, 2019) that acts as a major source of water supplies for domestic purposes in many parts of the world. Additionally, sinkholes constitute a significant hazard to public safety in built-up areas (Brinkmann et al., 2008). Their formation may cause collapses of structures and high material losses due to the destruction of buildings, roads and railways and other local infrastructure (Xua et al., 2017). The financial costs of dealing with the consequences of sinkholes are often very high. For instance, insurance companies in Florida received over 24.5 thousand claims for damages due to the formation of sinkholes, for a total sum of 1.4 billion dollars in the years from 2006 to 2010 (Kuniansky et al., 2015). Although a single sinkhole may be considered an event of local significance in terms of the scale of the phenomenon, it is of extreme importance in planning a given investment. It is reported that the combined effects of climatic conditions (atmospheric temperature and precipitation) and the urban sprawl shall result in the formation of sinkholes that shall also constitute a problem in the future. Therefore, it is of essential significance in the case of spatial planning and sustainable development (Strzałkowski, 2019).

On February 11, 2022, a phenomenon of sinkhole formation was observed near Wandevalgam village, Tehsil Kokernag, District Anantnag, Kashmir Himalaya within the Brengi stream. A crumbling sound and stir emerged out of the collapse of cap/roof rock at the stream bed that suddenly resulted in the formation of a sizable sinkhole in the area. Due to the progressive collapse and failure of the deformed steep side walls and continuous physical weathering, the diameter of the sinkhole further expanded on February 26, 2022. The noise of sinkhole formation and cap rock collapse has been heard at a distance of more than 200 m by the local people. The firsthand information about this unfortunate incident emerged through social media and, later on, through other sources of media reports and administration as well. This incident caused a worrisome situation in and around the local areas surrounding this place leading to illogical and unscientific rumors. It was found that the Department of Geology and Mining (DGM), Jammu and Kashmir, Srinagar had taken immediate cognizance of the situation at the site and reported that a sinkhole of sizeable dimension and swallowing more than 50 m^3/s (50 cusecs) of water discharge had formed in the area. The sinkhole thereby has disrupted the entire flow and left the downstream areas completely dry. Due to the drying of the downstream areas, the aquatic creatures (trout fishes) were left dead and devastated.

Pertinently, a similar type of sinkhole had developed during 1995 at about 50 m upstream from the present sinkhole as per the local reports. That time, the outlet of lost water was immediately found coming out at Achabal Karst Spring located downstream and on the other side of the mountain (~ 15 km away). That sinkhole later on slowly got plugged with sand, gravel, boulders and rock fragments. However, the outlet of the presently developed sinkhole was not immediately found by the authorities, even though the whole discharge of the stream was flowing into the sinkhole continuously for a couple of weeks. Further, no change in water levels in the wells and springs downstream of the sinkhole was observed for weeks. Pertaining to this, many speculations were also raised like (1) it might be that the swallowed water is lost to another underground channel/pond, (2) water is accumulating in some unknown underground reservoir or pond, (3) water is joining the underground water table directly, (4) the underground channel network or interconnection might have been disrupted during last decades and (5) what be the consequences and hazards of lost water and this type of phenomenon in the area. Therefore, this type of phenomenon further caused deep concerns and distressful situations among the local people and the concerned authorities in the area.

Thus, keeping the above discussion in view, the present study attempts to address these issues in the area. For this purpose, a detailed analysis of climatic and geological data along with field, geophysical and chemical tracer studies was carried to understand the mechanism and causes of sinkhole formation vis-à-vis its cap rock failure and to identify the outlet of the captured stream flow. A detailed analysis of available media reports, satellite images and other ancillary data sources was also carried out to document the associated hazards and risks of sinkhole formation and its future concerns in the area.

2 Study area

2.1 Characteristics of Brengi catchment

The Brengi catchment forms an important southwestern sub-basin of the Upper Jhelum River basin in Kashmir Himalaya. It covers a major part of the Anantnag District, UT: Jammu and Kashmir, India and lies between the geographical coordinates of 33°34′41.42″ N/75°20′18.59″ E covering parts of Survey of India (SoI), toposheet No. 43O/6 (Fig. 1). The area has rugged and undulating topography with high elevation structural ridges and

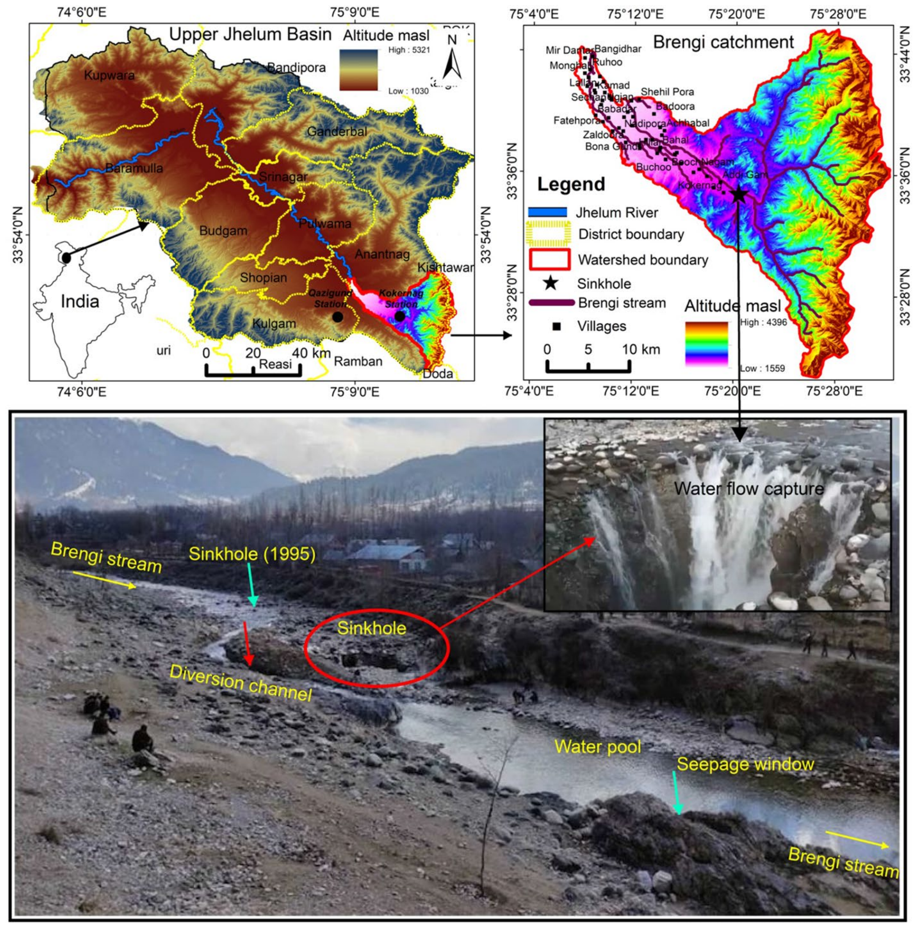

Fig. 1 Location map of sinkhole (black star) in Brengi stream. Top panel maps represent the watershed boundary of UJB and Brengi watershed. Field photograph shows the Brengi stream, sinkhole, diversion channel, water pool. Small inset photograph in field photograph, shows the water capture due to the sinkhole at the time of collapse

deep valleys. The elevation ranges from 1500 to 4400 m above MSL. In the area, the sinkhole developed at Kakawsar, Mirpora, Wandevalgam village, near Kokernag Tehsil, with coordinates 33.57° N and 75.33° E. It is located at an elevation of 1957 m MSL, within the river bed of the Brengi stream. The Brengi stream is one of the major tributaries of the Jhelum River in Kashmir Himalaya. Brengi stream possesses a dendritic drainage pattern and flows in north-westerly direction after originating from the Pir Panjal Mountain range. The stream is the main source of water for irrigation and other domestic purposes for the local populace, besides breeding habitat for trout fishes and other ecosystems in the area. It is formed by the confluence of Nowbugh stream, Ahlan Gadol stream and Daksum stream. Nowbugh stream originates from the glaciers of Margan Top-Kishtwar side and Daksum stream from the glaciers of Sinthan in Anantnag district. It flows for a total of 30 km before joining the Jhelum River at Haji Danter, Anantnag. The Kokernag area is also popularly known as Brengi valley due to Brengi stream.

2.2 Climate and geology of the area

In the study area, a typical temperate climate is prevalent (Mir & Gani, 2019) with temperatures varying between a monthly mean maximum of 32 °C in July and a minimum of − 15 °C in January with an annual average of 9.5 °C (Mir, 2018). The mean annual precipitation is reported to be about 992 mm, average rainy days of about 74 and the highest rainfall of 210 mm recorded in March and the lowest (i.e., 48 mm) in November (Mir & Jeelani, 2015). The precipitation is received mostly in the form of rain and snow. The seasonal snowfall covers a considerable area of the study area during the winter season. The snow cover melts in the spring season to feed the groundwater and streams for the rest of the year (Mir, 2018; Mir et al., 2016).

The regional geology of the study area is characterized by a complete stratigraphic succession of rocks from Paleozoic to Quaternary period. The main lithounits exposed are limestone, basalt, shale, arenite, siltstone, greywacke, slate, phyllite, etc. The details of the various lithounits are given in Table 1. Structurally, the study area falls under the Nappe Zone of Kashmir having the general strike of NW–SE trend. The strike of bedding is NW–SE to NNW–SSE with moderate-to-high dips in either direction. The Pre-Pleistocene rocks are strongly folded with axes oriented in the NW–SE direction. The whole sequence of rock formations is folded into a major anticline and syncline. The bed rock dips generally range between 25° and 75°. However, the beds are also locally vertical and over-folding is common in the high limestone ridges of the area. The trend of the fold axis and major lineaments giving the surficial expression of internal geological structures (faults, shear zones) is also in the NW–SE direction. However, certain lineaments reflect the occurrence of cross structures (may be major faults) in the area. The geological map of the rock formations of the area is shown in Fig. 2.

3 Materials and methods

In this study, data from several sources including the literature, ancillary and media reports, geological maps, Survey of India maps, Satellite and Google Earth images and available data from metrological stations have been used. Just after the formation of sinkhole on February 11, 2022, a preliminary survey of the literature or information was carried out and, consequently, the data were collected from different sources including existing reports, newspapers, district administration, local people, etc. Subsequently, on February 14, 2022, a detailed field survey was carried out to collect information from different parts of the area for detailed assessment of the situation and to understand the possible reasons behind the abrupt collapse of limestone streambed (cap rock) and sinkhole development in Brengi stream. Observations and data in the context of exposed lithology and structural fabric attributes (bedding, fractures, joints, shear zones, faults) were collected. The coordinates and dimensions of the current sinkhole, coordinates of the previous sinkhole and points with high seepage were recorded. The volume of the water pool at the sinkhole location just before the failure was estimated using the leftover marks on the rocky outcrops surrounding it. The length and breadth of the failed water pool were determined using the measuring tape, and an average depth was used to measure the volume of the lost water pool. A similar methodology was adopted for

Table 1 Geological stratigraphic succession of the rock rocks of the area (modified after GSI, 2012)

Lithology	Formation	Group	Age
Alluvium, moraine, scree	Quaternary		Holocene
Loamy silt, thin sandy bands and loess sediments	Dilpur	Karewa	Pliocene to early Pleistocene
Limestone, slate, sandstone	Wumuh	Vihi	Jurassic
Limestone, shale, sandstone, dolomite	Khunamuh, Khreuh and Wuyan		Triassic
Shale, limestone	Zewan		Late Permian
Basalt, andesite	Panjal volcanics	Panjal	Early Permian
Arenite, diamictite, pyroclast, phyllite with ash beds	Agglomeratic slate		Late Carboniferous to early Permian
Sandy shale, siltstone, quartz arenite	Fenestella shale	Lidder	Middle Carboniferous
Calcareous arenite, shale, limestone	Syringothyris limestone		Early Carboniferous
Orthoquartzite with shale bands	Muth quartzite	Gugaldhar	Devonian
Variegated shale, arenite, conglomerate	Margan		Ordovician to Silurian
Shale, slate, arenite, limestone	Karihul	Hapatnar	Middle Cambrian
Siltstone and shale	Goaran		Early Cambrian
Arenite and greywacke	Matehund		
Siltstone, shale, greywacke	Lolab	Pohru	

measuring the volume of water in a newly formed water pool, after diverging the stream flow toward downstream of the current sinkhole, located at a distance of 15 m.

The discharge flow in the divergent stream and a small stream flowing into the sinkhole along two sides was also measured using the velocity area method, Eq. (1). These three measurements of water flow were added up to get the total water discharge in the Brengi stream.

$$Q = V \times D \times W \tag{1}$$

where Q = discharge in m^3, V = Velocity per unit time of water flow, D = Unit depth of water column in the stream in m, and W = Unit width of the cross section of stream in m.

Furthermore, the ground magnetic surveys were also carried out at the interval of 1 m using the Proton Precession Magnetometer (PPM) across the Brengi River at the sinkhole location and the immediate vicinity of the sinkhole to analyze the magnetization factor and to detect variations in the magnetic field intensity. For this purpose, two profiles, one on the upstream and downstream of the sinkhole, were selected for the survey, respectively. The magnetic intensities were also analyzed at random points for data profiling and calibration. The diurnal variations were analyzed before interpreting the profile to create smooth data collection at the sinkhole.

To determine the outlet of the sinkhole, a tracer study was carried out. For this purpose, 10 kg of methylene blue powder was injected into the sinkhole at 11.30 am and 12.00 pm on 21.02.2022 (Payne, 2000; Trillat, 1899). Methylene blue (C.I. 52015) has excellent visibility in soils and is a commonly used dye that also exhibits antioxidant, antimalarial, antidepressant and cardioprotective properties (Table 2). Observation sites (springs and tube wells) were established downstream of the sinkhole at Soaf-Shalli (6 km downstream of the sinkhole on the right bank of river), Adigam (2.5 km downstream of the sinkhole on the left bank of the river), Hillar (11 km downstream of the sinkhole on the left bank of the river and four springs at Achabal (16 km downstream of sinkhole) as shown in Fig. 3.

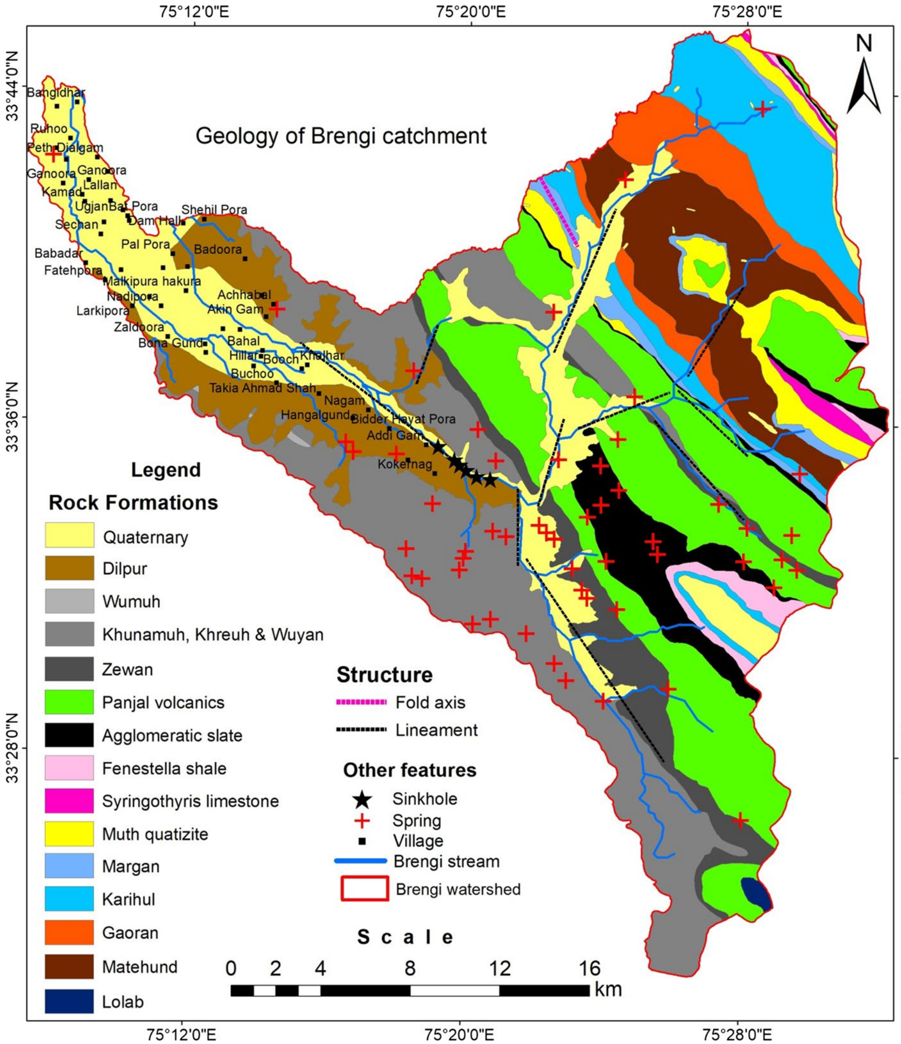

Fig. 2 Geological map of the Brengi catchment showing the distribution of major lithounits and carbonate rocks, karst springs and sinkholes. The map also shows the location of major lineaments and fold axis. The lineaments have been derived from DEM, Google earth imagery and SoI toposheet

Water samples, at regular intervals, were collected from all the selected control points before and after the dye injection. Once the dye was injected in two slots 11:30 am and 12:00 noon on 21.02.2022, the samples were collected from control points at regular intervals for the next 24 h. About 120 water samples (30 pre-injection and 90 post-injection) were collected from control points for tracer detection using UV–Vis Spectrometer (Trillat, 1899).

In order to understand the climatic regime in the area, an analysis of the climatic data was carried out. The climate data of Qazigund and Kokernag meteorological stations were collected from IMD for a period from 1977–2015 and 1980–2015, respectively. Furthermore, the detailed geological maps were collected from the Geological Survey of India web-server

(Bhukosh). The data on spring inventory were generated from Survey of India toposheets and Google Earth imageries. The ALOS-PALSAR DEM was downloaded from the website https://asf.alaska.edu/ to understand the topography and morphology of the area. The high-resolution ALOS-PALSAR is radio-metrically corrected DEM with a spatial resolution of 12.5 m provided from the Alaska Satellite facility. The DEM was also utilized to extract watershed, stream network and drainage network of the area. Sentinnel-2A scenes with a spatial resolution of 10 m covering the whole study area were also used (Ahmed et al., 2022). The data were downloaded from the Copernicus internet hub of European Space Agency (ESA) to analyze the water flow in the Brengi River before and after the formation of the sinkhole (pre- and post-sinkhole formation). To understand the downstream land use and land cover of the study area, the LULC map of Environmental Systems Research Institute (ESRI) with a spatial resolution of 10 m was downloaded from the website https://www.arcgis.com/ website. The LULC classes were identified according to the legend given by (ESRI, 2021). The accuracy assessment of the LULC indicating an accuracy of 86.58% was also done (Macleod & Congalton, 1998; Ahmed et al., 2021; Imdad et al., 2022; Sahana et al., 2019). Subsequently, all the data were processed and analyzed in the GIS environment. The work flow of methodology is shown in Fig. 4.

4 Results

To conduct a preliminary assessment and furnish a detailed report specifically describing the causes, mechanism, hazards and remedial measures of sinkhole formation in the Brengi stream, a detailed analysis of available data in conjunction with field investigations, geophysical and tracer studies was carried out in the area. The observations and results are described in detail below.

4.1 Field survey

To understand the process of caving in of Brengi stream and sinkhole development, a field investigation was carried out in and around the Brengi sinkhole. At this location, the stream along its course downstream is surrounded by steep structural hills consisting mainly of massive and thickly bedded Triassic limestone with very thin intercalations of shale on its right bank, whereas the left bank forms a high terrace (> 10 m height) comprised of Quaternary sediments. The limestone is a very fine carbonate mosaic and mostly pure consisting of more than 80% of calcite minerals. It also contains small proportions of fossil fragments and ferruginous, insoluble grains. However, impure limestone consisting of 15–90% dolomite is also found at certain locations around. Horizons of shale and sandstone of thickness up to 5 m are also common throughout the succession.

At the sinkhole site, the limestone is massive and thickly bedded (0.30–2.00 m thick), dark bluish–green in color, with very thin yellowish shale partings (0.10 m thick) representing the bedding planes. The limestone beds are highly brecciated, deformed and folded

Table 2 Characteristics of the tracer chemicals used in this study

Dye class	Commercial name	C.I. generic name	C.I. number	Hue (color)	Source
Thiazine	Methylene blue	C.I. Basic Blue 9	52015	(Bright) greenish blue	Trillat (1899)

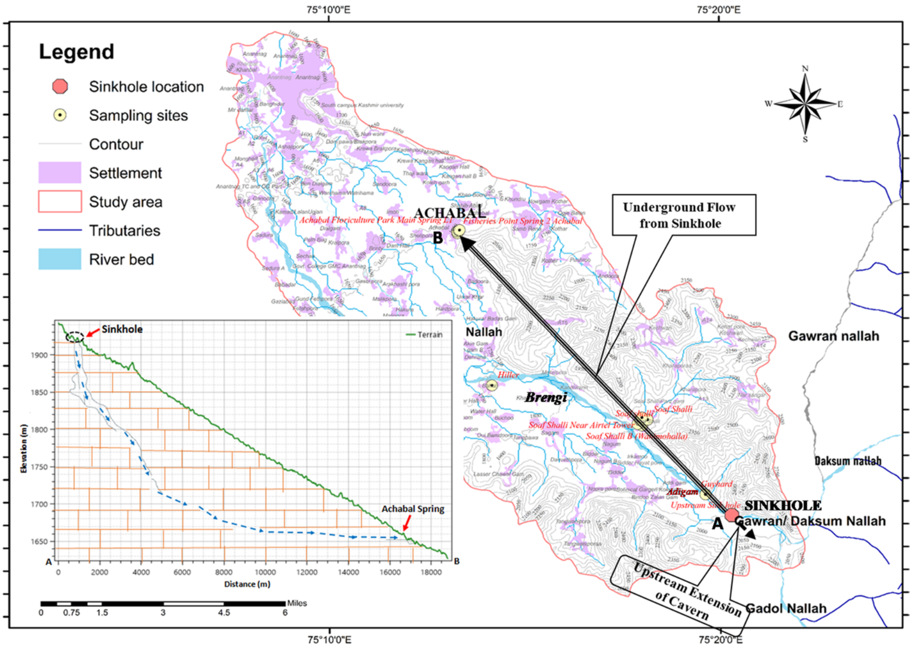

Fig. 3 Map showing location of the sample collection sites during pre- and post-tracer injection in the area. The inferred underground flow path of the sinking water and its resurgence is depicted along the profile line A–B on the map

at many places at and around this site. The deformational features are very well preserved at the limestone outcrop lying toward the western and eastern parts of the sinkhole. Toward the western side of the sinkhole, a large limestone outcrop of about 10 m in height and about 25 m in length is exposed. The enlarged fractures and caverns formed due to prolonged chemical action are well preserved. The water-level markings representing a large pool of water (before sinkhole development) at the site were found well preserved on the limestone outcrop. The average depth of the water column was estimated to be about 1.5 m, whereas the length and width were measured to be 40 m and 20 m, respectively. Thus, the total volume of the water column at this site was estimated to be more than > 80 m^3 before the collapse of its stream bed. Downstream, at a distance of > 15 m from the current sinkhole, another water pool was formed due to the accumulation of diverged stream flow toward the right bank of the stream. The depth of the water column in this pool was found to be 3–4 m with a length and width of 20 m (Fig. 5a–i). During the field investigation, 5 more relatively smaller sinkholes were found both upstream and downstream lying nearly in a linear pattern for the current sinkhole (Fig. 2). The linear alignment of the sinkholes suggests a possible underground connection via a major cavern. Water diverted from the major sinkhole was observed to seep through these smaller sinkholes.

The sinkhole is found to be vertical almost, a funnel-shaped shaft. It is narrowing down toward the bottom and is lost to depth through a small cave opening (1–2 m diameter) at the bottom. The dimensions of the sinkhole were measured to be 12 m in diameter and > 20 m in height. The exposed limestone bedrock near the sinkhole is highly brecciated, fractured, compressed, weathered and deformed. Half of the sinkhole on

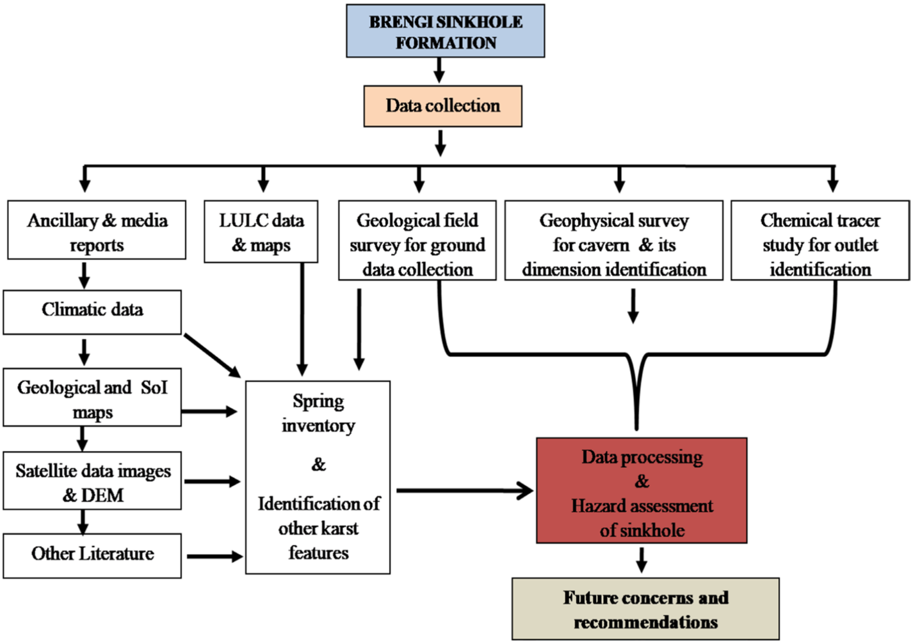

Fig. 4 Workflow of the methodology adopted in the study

the left side was highly brecciated and broken, whereas more than half of the wall was intact showing a wedge type of failure/dislodgement of rock block due to the collapse of cap rock. A major rock block present at the middle part of the sinkhole partly dislodged and displaced shows the presence of several sets of joints (3 sets) and fracture planes (Table 3). The massive collapse of sinkhole walls has produced large breccia blocks and rubble in the sinkhole. The spacing between the joint and fracture planes varies from 0.01 to 0.61 m. At this site, the bedding planes are oriented in the NW–SE direction dipping toward the east at 60–70°. A major vertical fracture plane running almost parallel to the bedding plane was also present. The fracture plane is enlarged due to the prolonged chemical action of the circulating water over a long time. The same enlarged fracture plane was continuing and present on the limestone outcrop near the newly generated water pool (> 15 m downstream of the sinkhole).

The fracture plane was found to act as a major infiltrating window of the stream flow into the underground tunnel at this site. Additionally, the limestone basement rocks forming the Brengi stream bed were overlain by a thick overburden cover of transported alluvial material, varying in thickness from 0.61 m toward the right side (eastern margin of sinkhole) to 2–3 m toward the left side (western margin). The overburden material was comprised of boulders of basaltic rock with diameters ranging from 0.30 to 1.00 m. In predominance, the boulders form a higher proportion (> 60%) followed by gravel, pebbles and sand. Toward the eastern side of the sinkhole, the thicker overburden material was found to have been deposited within a deep channel grooved within the limestone bedrock probably due to the extensive and focused chemical weathering by the concentrated stream flow (Fig. 6a–f).

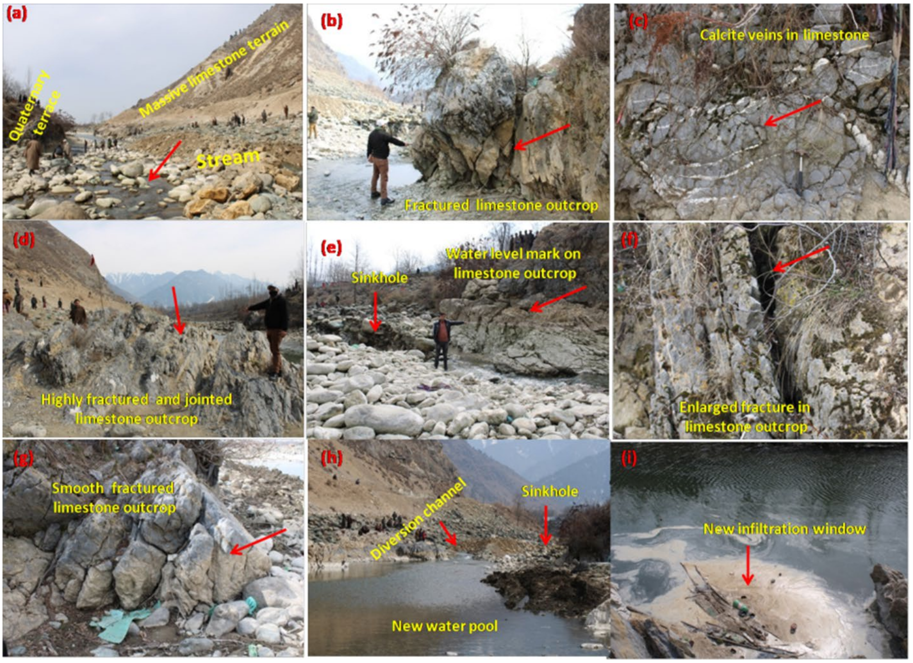

Fig. 5 Field photographs showing **a** massive limestone and quaternary deposits, **b** fractured and brecciated limestone outcrop, **c** calcite veins indicating shearing in limestone outcrop, **d** highly fractured and deformed limestone outcrop; **e** previous water-level mark of lost water pool on limestone outcrop, **f** enlargement of fracture planes in limestone outcrop due to mineral dissolution, **g** smooth surfaces and edges created due to prolonged chemical action of water on limestone outcrop, **h** new water pool formed below the diversion channel, **i** seepage of accumulated water down through new infiltration window created in the water pool near limestone outcrop at the sinkhole site in the Brengi stream

4.2 Geophysical survey

The sinkhole in the riverbed of the Brengi stream is a part of an unknown major underground and interconnected network of channels. This is inferred from the fact that the old sinkhole developed in 1995 (about 50 m upstream of the current sinkhole), the current sinkhole and the new infiltration window (about 50 m downstream from the current sinkhole) are aligned on a single line controlled by a major fracture and bedding planes of limestone trending NW–SE directions dipping toward NE. At this location, the Brengi

Table 3 Structural disposition of Triassic Limestone near the sinkhole site in the Brengi stream

Data type		Strike	Dip amount	Dip direction
Bedding	S0	320	66	50
Joint sets	J1	340	70	70
	J2	0	60	270
	J3	100	72	10
	J4	40	2	320
Fracture	Fr	95	77	185

stream is running almost parallel to this structural disposition of the bedrock. Based on these observations, the occurrence of a single channel (dimensions not known) running underground (> 25 m depth) and draining the swallowed water could not be ruled out. This underground channel was expected to continue downward till Achabal spring where the water emerges. This observation was also supplemented by the tracer test results of the current study as well as previous studies (Bhat et al., 2021; Coward et al., 1972).

During the field survey, ground magnetic surveys (PPM studies) were carried out across the stream to estimate the probable depth as well as the dimensions of this underground channel at and around the sinkhole site. The data were analyzed to estimate the magnetization factor and the variation of total magnetic intensities produced by the hydraulic activities and martitization processes of the subsurface cavern material formed at the river. The results indicated that the subsurface cavern is associated with magnetic minima which is due to the dissolution processes, resulting from the carbonation or oxidation of rock material along the cavern (Fig. 7). At Profile 1 upstream of the sinkhole, a variation of 13 nT between the magnetic minima and maxima was found. The cavern was found at the range of 50,881–50,884 nT with a total length of 3 m at the sinkhole location and flowing toward the NE of the stream. Similarly, Profile 2 shows the magnetic variation of 14 nT between magnetic minima and maxima downstream of the sinkhole. At this site, the cavern was found at the range of 50,884–50,887 nT with a total length of 2 m at a 6 m distance from the sinkhole location. Thus, according to these results, the underlying cavern is found to be about 100 m long downstream. However, in this direction, detailed ground magnetic surveys and gravity surveys are recommended to estimate the absolute depth and mechanical behavior of the subsurface cavern system in the area. The detailed potential geophysical surveys with convenient data methods and interpretations shall reveal the subsurface details of karst topography in the region.

4.3 Chemical tracer study

The chemical tracer study was carried out to ascertain the path of the underground water flow sinking into the sinkhole. The tracer tests were conducted on 21.02.2022, and subsequently, the samples were collected at different locations downstream of the sinkhole for both pre-and post-injection periods ranging from 2 to 24 h, respectively. During this study, about 120 water samples (30 pre-injection and 90 post-injection) were collected from the selected control points [i.e., 4 locations at Achabal, i.e., (1) Achabal Fisheries Spring, (2) Achabal Floriculture, (3) Park Main Spring L1 and (4) Achabal Floriculture Park Spring L2]. Out of a total of 90 samples collected after post-injection, only 9 samples showed the presence of tracer chemicals. The pre-injection water samples collected at 8:00 am as well as the post-injection samples collected from 3:00 to 8:00 pm showed no signs of traces. Only the samples collected from 9:00 to 11:00 pm at Achabal (Achabal Fisheries Spring, Achabal Floriculture Park Main Spring L1 and Achabal Floriculture Park Spring L2) showed the tracer chemicals. Similarly, the samples collected from 7:00 am till 12:00 m (next date) also did not show any traces. All 9 samples that showed the presence of tracer chemicals were collected from Achabal area or springs. However, it is essential to note that no traces were detected from the samples collected at Soaf-Shalli, Adigam and Hillar sites. The appearance of traces at the outlet shows an approximate residence time of 12–14 h of sinking water from point of injection (Sinkhole site) to Achabal area or springs over a distance of about 16 km. These

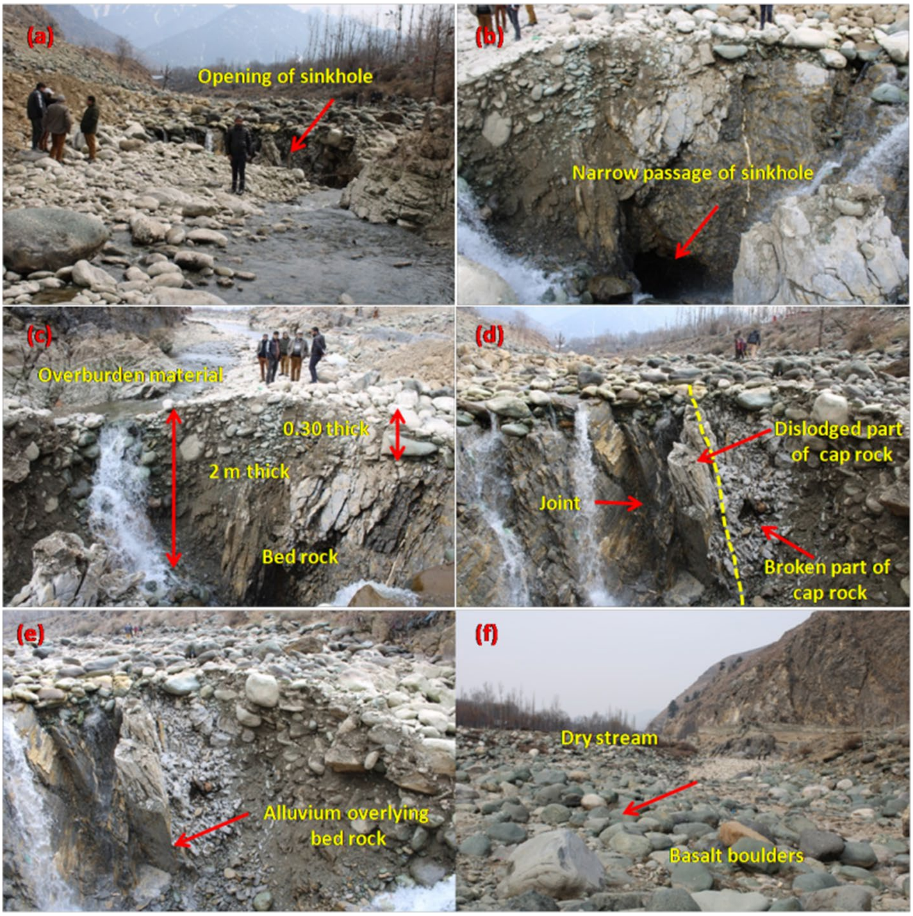

Fig. 6 Field photographs showing **a** opening and caving in of sinkhole roof cap rock, **b** narrow passage or swallet of sinkhole, **c** thickness and composition of overburden alluvial material, **d** intact and deformed/broken portions of cap rock; dislodged part of the cap rock, **e** dense basaltic boulders and sand overlying the cap rock, **f** widespread basaltic boulders over the stream bed near the sinkhole site in the Brengi stream

results therefore indicated an average velocity of ~ 1.3 km/h of the water flow during the underground movement from the sinking site to the outlet. Moreover, it is very pertinent to mention that the outlet of swallowed water by sinkhole on February 11, 2021 should have also been released through these identified outlets. But, the identification of that surplus discharge was either not witnessed or monitored timely in the area. The detailed results are given in Table 4 and Supplementary data. Overall, the tracer detection results suggested that the outlet of captured stream flow by the sinkhole was located at the Achabal area or Achabal karst springs. Although the karst springs at Achabal contribute too significantly and dominantly to the outlet of the swallowed Brengi stream discharge, at the same time it did not rule out other possible outlets in the adjoining areas. To identify all the outlets of the sinkholes and the interconnection of the underground channel network, a detailed study in this direction is recommended in future in the area.

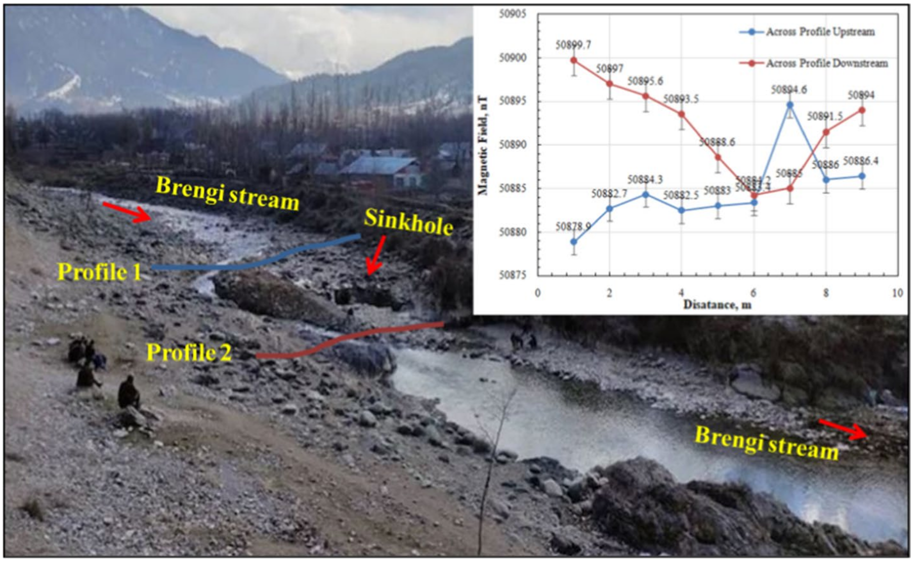

Fig. 7 Variation of magnetic field showing the magnetic anomalies at Profile 1 and Profile 2 across the Brengi stream at the sinkhole site

The typical absorption spectrum of the analyzed water samples showing the presence of tracer chemicals is shown in Fig. 8.

5 Discussion

An understanding of the prevailing climatic conditions and the geological setup is very essential to understand the mechanism of karstification or sinkhole development. The abundance of water and unprecedented solubility of rocks are the primary factors required for the karstification of any area. Therefore, in this study, a preface understanding of the climatic regime and geological setup of the area was carried out as described briefly henceforth.

5.1 Climatic regime

Karst development is strongly influenced by climate via temperature regime and available moisture balance. In order to understand the temperature and precipitation regime in the study area, the meteorological data from the nearest Qazigund and Kokernag stations were analyzed. The Qazigund station lies in the Sandren basin lying adjacent to the Brengi basin, whereas the Kokernag station falls in the Brengi catchment itself and is very close about 5 km away from the Sinkhole location. The analysis of temperature data of Qazigund station from 1977 to 2015 showed that the mean T_{max} is varying from 17.5 °C (1990) to 20.6 °C (1996) with an average of 19.2 °C, whereas the mean T_{min} varies from 4.8 °C (2006) to 7.1 °C (2014) with an average of 6.4 °C. The mean T_{min}

Table 4 Results of detection of tracer chemicals in water samples in and around Achabal area (karst springs) and other selected areas

S. no.	Sample ID	Place	Latitude	Longitude	Altitude M asl	Time	Tracer detected
1	AFPS13	Achabal Floriculture Park Main Spring L1	33.68212	75.22232	1634	9:00	Yes
2	AFPS13a	Achabal Floriculture Park Spring L2	33.68234	75.22195	1637.88	9:00	Yes
3	AFS14	Achabal Fisheries Spring	33.6813	75.22144	1667.79	9:00	Yes
4	AFPS14	Achabal Floriculture Park Main Spring L1	33.68212	75.22232	1634	10:00	Yes
5	AFPS14a	Achabal Floriculture Park Spring L2	33.68234	75.22195	1637.88	10:00	Yes
6	AFS15	Achabal Fisheries Spring	33.6813	75.22144	1667.79	10:00	Yes
7	AFPS15	Achabal Floriculture Park Main Spring L1	33.68212	75.22232	1634	11:00	Yes
8	AFPS15a	Achabal Floriculture Park Spring L2	33.68234	75.22195	1637.88	11:00	Yes
9	AFS16	Achabal Fisheries Spring	33.6813	75.22144	1667.79	11:00	Yes
10	SS1-10	Soaf-Shalli	33.61317	75.30224	1855.99	–	No
11	AG1-7	Guyhard (Adigam)	33.58596	75.327	1899.04	–	No
12	HL1-11	Hillar	–	–	–	–	No

The absorption spectrum of methylene blue of few samples is shown in Fig. 8

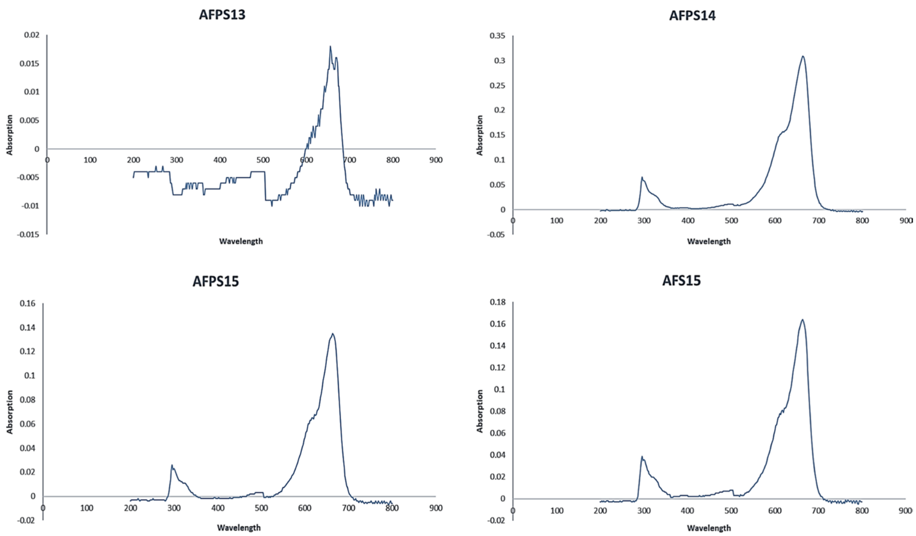

Fig. 8 Absorption spectrum of methylene blue of water samples collected at Achabal Floriculture Park Main Spring L1 (AFPS13), Achabal Floriculture Park Main Spring L1 (AFPS14), Achabal Floriculture Park Main Spring L1 (AFPS15) and Achabal Fisheries Spring (AFS15), after the injection of chemical tracers in the area. For details, refer to Table 4

generally remains below freezing during the months from November to February in the area. The mean sum of precipitation varies from 751.3 mm (2001) to 1902.6 mm (1996) with an average of 1212.1 mm (Fig. 9a).

Similarly, the climate data from Kokernag station analyzed from 1980 to 2015 indicated that mean T_{max} is varying from 15.8 °C (1995) to 20.1 °C (2001) with an average of 17.9 °C, whereas the mean T_{min} varies from 4.4 °C (1986) to 7.7 °C (2006) with an average of 6.4 °C. The mean T_{min} generally remains below freezing during the months from November to February in the area. The mean sum of precipitation varies from 579.5 mm (2000) to 1542.0 mm (2014) with an average of 1047.8 mm (Fig. 9b). The climate data analysis, therefore, indicated the prevalence of a suitable temperature and precipitance regime in the area for karst development.

5.2 Geological setting

The study area is characterized by mature 2nd-order topography, with valleys and hills marking structurally anticlines and synclines, respectively. The development of karst topography is highly favored by these topographical and structural features, wherein the development of karsts (sinkholes, caverns) generally occurs largely toward synclines than toward the anticlines (Bhat et al., 2021). The present course of the Brengi stream toward and along the hillside leads to water disappearance through karst sinkholes significantly at many places from Adigam to Achabal (Bhat et al., 2021). Several sinkholes of varying dimensions have been noticed at various places along this course of the Brengi stream, e.g., near Adigam, Devalgam and Gadol villages (Jeelani et al., 2015). Similarly, the occurrence of the higher number of springs associated mainly with the

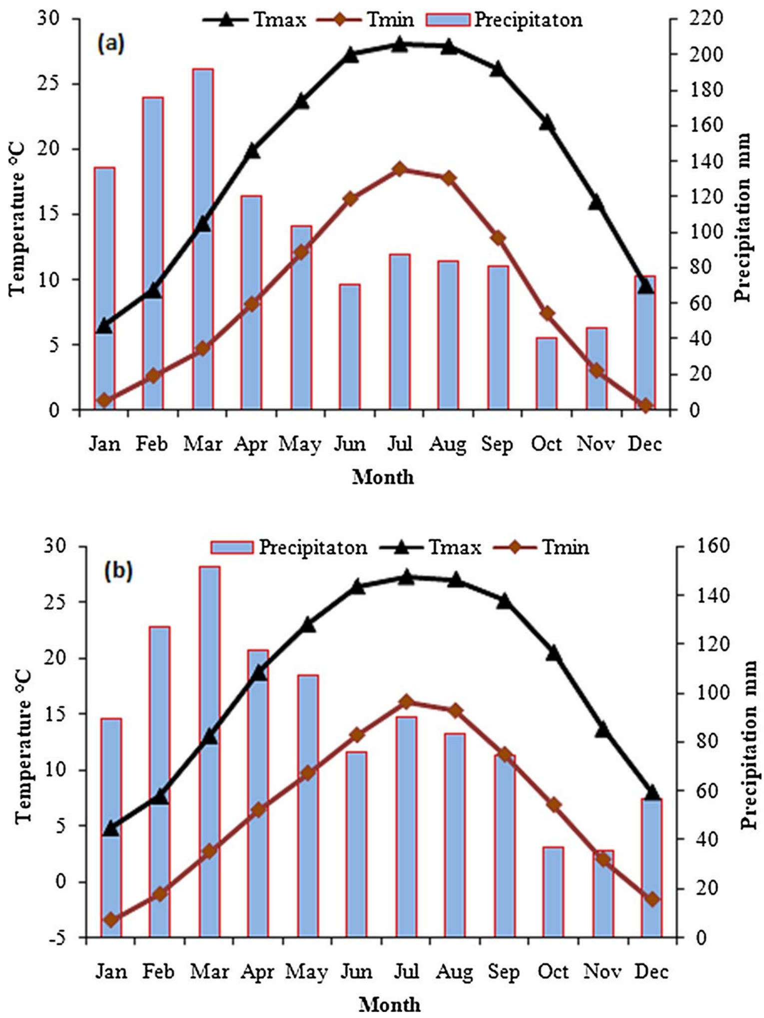

Fig. 9 Monthly variation of average temperature (T_{max} and T_{min}) and precipitation at **a** Qazigund station (1977–2015) and **b** Kokernag station (1980–2015) near and within the Brengi catchment in the area

Triassic limestone as well as Panjal volcanics and agglomerate slates indicates the inherent lithological as well as structural control on its occurrence in the area. The Triassic limestone and Panjal traps are fractured and have high inherent hydraulic conductivity (*K*) (i.e., 6 m/day for the fractured Traps and up to 1000 m/day (for the karstified limestone), whereas the overlying Karewas and alluvium deposits have low *K* values (Shah & Jeelani, 2016). The low *K* values for Karewa (1–10 m/day) and alluvium (0.1–5 m/day) are due to the presence of fine and compact detrital sediments (sand, silt and clay). Thus, the karst springs normally emerge from Triassic limestones along the foothills of Pir Panjal in contact with alluvium deposits (Jeelani, 2008).

The correlation between the occurrences of springs and lithological units in the area indicated that the majority of the springs are associated with Triassic limestone rocks representing karstification in the area. Many of these characteristic karst springs are aligned along the major geological structures and lineaments such as bedding planes and fault/shear zones (Fig. 2). Besides, a few springs are also associated with other rock types such as Panjal volcanics and agglomerate slates in the area. The occurrence of these springs can be clearly attributed to the presence of major structural discontinuities or structural fabrics such as major faults, shear zones and joints. The surface drainage pattern of the Brengi stream is also dominantly controlled by the structural disposition of the bedrocks in the area (Fig. 2). Few springs are also observed emerging through the overlying Quaternary sediment cover in the area. Thus, from these observations, it can be inferred that in addition to well-developed surface drainage, an underground interconnected system of drainage conduits or caves is also present and may be extending to shallow depths or depths of hundreds of meters or even more in the area. The well-fractured, faulted, jointed and sheared, soluble and dense limestone rock formations near the surface and interconnected underground stream network with good surface vis-a-vis groundwater circulation provide suitable conditions to promote karst and sinkhole development in the area. The interconnected underground caverns facilitate the movement of water that sinks into the ground via the sinkhole or other openings, to appear in the form of springs. However, the flow characteristics of these springs are dominantly controlled by geological structures (major fault and shear zones) that are acting as preferred paths from recharge to outlet points. Such processes in the long run create underground channels/drainage, fissures, sinkholes and sinking streams and represent the karst landscape and topography in the area. The occurrence of a large number of springs (both cold and warm) and the presence of other surface karst features (such as caverns, conduits, shafts, Karren fields and pits) are the prominent surficial karst features in the area (Jeelani et al., 2018; Shah et al., 2018).

5.3 Causes and mechanism of sinkhole formation

There are several possible reasons for the development of sinkholes, but the most common, by far, is the collapse of caves in limestone bedrock by the agency of weakly acidic groundwater and the dissolution of the mineral calcite. The limestone, chemically composed of calcite mineral ($CaCO_3$), easily dissolves over time in the presence of carbonic acid (HCO_3), formed as a result of the reaction between the water (H_2O) and the atmospheric carbon dioxide (CO_2). However, the dissolution capability of H_2O with respect to $CaCO_3$ is related directly to its CO_2 content in the system. The CO_2 is derived directly from the atmosphere through precipitation as well as from the biogenic sources at the surface and subsurface environments (Waltham et al., 1997; Ford & Williams, 2007). The chemical reaction between CO_2 and H_2O to produce HCO_3 (a weak acid) further reacts with carbonate minerals and results in carbonation processes (Goldscheider et al., 2020).

$$\underset{\text{air}}{CO_2} + \underset{\text{water}}{H_2O} \rightarrow \underset{\text{carbonic acid}}{H_2CO_3} \tag{2}$$

$$\underset{\text{calcium carbonate}}{CaCO_3} + \underset{\text{carbonic acid}}{H_2CO_3} \rightarrow \underset{\text{calcium ion}}{Ca^{2+}} + \underset{\text{bicarbonate ion}}{2HCO_3^-} \tag{3}$$

Carbonation primarily occurs in wet, moist climates and dissolves rocks both on and beneath the surface. Small amounts of dissolved CO_2 in rainwater provide weakly acidic groundwater which slowly dissolves limestone along fractures. This process simultaneously weakens the rock and removes the chemically weathered materials over time. The area has a temperate climate with plenty of precipitation. The climate data analysis revealed a moderately warm and suitable temperature regime (average temperature varying from 6–15 °C) particularly from March to September. The favorable temperature promotes chemical weathering processes and the dissolution of carbonate lithology. A moderate to heavy precipitation (average annual precipitation of > 1000 mm) further magnifies the chemical dissolution processes of the carbonate rock at the suitable prevailing temperature regime. Over long periods of geologic time, these slow rates of dissolution are capable of making gigantic underground caverns. During the formation of a cavern or cave slowly and by enlarging, the strength of the cap rock is reduced sufficiently to hold the weight of overlying rock strata and the overburden material. The dissolution of limestone rocks involves interrelated air (gas), water (aqueous) and rock (solid) phases in the chemical environment. The process of carbonation is further influenced by the temperature, water flow, vegetation, pressure and partial pressure of CO_2, Ph and other ion concentrations in the system (Smith & Atkinson, 1976). For instance, cold water has more dissolved $CO_{2,}$ whereas in deeper water, more CO_2 is absorbed and hence is more acidic in nature. The acidic water infiltrating along the existing joints, fractures and bedding planes in the limestone bedrocks develops the secondary and tertiary porosities and subsequently leads to the development of vertical and horizontal karst drainage and other related features such as sinkholes (Sheen, 2000; Field, 2002).

The carbonate rocks found in the area are more than 250 million years old. Over time the soluble rocks have been easily dissolved by the inflowing meteoric water through chemical action under favorable climatic regimes. This phenomenon is manifested through the presence of a large number of karst features present in the area (Shah et al., 2018; Jeelani et al., 2018). The high discharge springs like Kokernag, Sheerbag, Panzathnag, Malaknag, Verinag and Achabal emerging from limestone terrain is also the testimony of such phenomenon and underground karst landscape. In this area, the strike of the highly jointed limestone beds and primary structural discontinuities (fractures) is mostly along the course of the Brengi stream, i.e., NW. Therefore, these joint and fracture planes are considered to be the main avenues through which the water has been penetrating and causing the dissolution of rocks by chemical weathering. These joints are regional in scope and may have been originally formed during the different stages of Himalayan orogeny that warped and uplifted to the present elevation. The fracture apertures have increased in size and have developed into a complex system of underground interconnected caverns over a long period of time. The presence of unconsolidated highly permeable river bed material also favors the higher dissolution of limestone rocks and weakening of the bedrock/capping.

Overall, the findings suggested that the sinkhole was developed by the chemical dissolution of Triassic limestone followed by the collapse of the roof cap. The preexisting underground interconnected system of caverns and continuous dissolution of the bedrock from the surface has taken place and caused the collapse of unsupported sediment above the underground hole. The presence of extensive sedimentary and other structural features has been facilitating rapid chemical weathering and dissolution processes in the limestone. In addition to the chemical weathering of the cap rock, its collapse might have been aggravated by the huge weight of the thick overburden alluvial material and the deep-water column above it before the collapse. Approximately 3-m-thick overburden material consisting mainly of basaltic boulders of high specific gravity (2.7–3.3 g/cm^3) and large water volume (> 80 m^3) was observed to be present just before the development of the sinkhole. It is because the bedrock is intact toward the side with thin overburden material. The presence of bedding, fracture and joint planes is found to have also facilitated cap rock collapse and slip-by-wedge type of failure mechanism (Fig. 10a, b). Thus, it is suggested that the development of this sinkhole has involved a roof rock failure into the underlying cave within the Triassic limestone rock formation due to the thinning of the original cave roof to the point of failure over a long period of time (i.e., millions of years). The failure was sudden, with almost vertical walls and floor sloping down into an open cavern. The sinkhole is therefore classified as a "Collapse Sinkhole."

5.4 Hazard assessment of sinkhole formation

Due to the sudden development of the sinkhole, the entire discharge in the Brengi stream was disrupted and lost to the underground channel/cavern network. This resulted in the loss of threshold environmental base flow of the stream and drying of the downstream areas. As per the initial reports of the DGM, > 50 m^3/s (50 cusecs) of water were lost to the sinkhole. Consequently, the downstream stretch of the stream dried up completely and disturbed the downstream hydroecology of the watershed. The Landsat satellite image clearly depicts the active stream flow and its disappearance after the sinkhole development in the area (Fig. 11). Since the stream is the main source for multiple irrigation canals, drinking water schemes, breeding ground for trout fish and flows through various habitations in the area, the event posed risks of varying severity. The aquatic life downstream was left dead creating panic and threats about the future consequences of the incurring disaster among the residents.

Field photographs showing the drying up of the downstream area of the Brengi stream are shown in Fig. 12a, b. Although the concerned district administration created a diversion channel immediately to prevent the water loss and restore the flow in the downstream areas, the diverged water was accumulating in the new water pool (about 50 m downstream) and

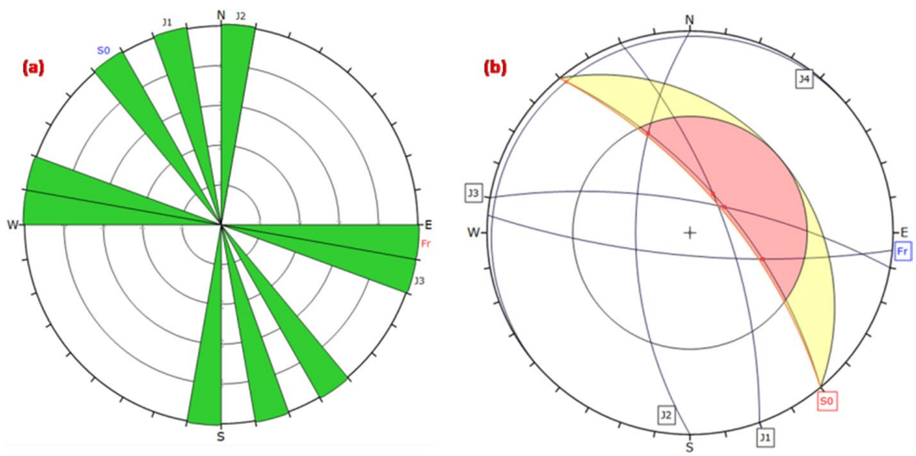

Fig. 10 Rose diagram and stereo-plot showing **a** the general orientation of structural data and **b** wedge type of failure/during the collapse of cap rock of sinkhole in the Brengi stream

seeping through the weathered and fractured riverbed leaving the downstream areas still completely dry. A significant portion of water (approximately 30%) was still being lost to the sinkhole. As per our estimates, a total water discharge of ~ 15.03 m^3/s was being lost to the underground karst system at the site continuously for a couple of weeks (Fig. 12c). As per the local people, Brengi stream has a history of sinkholes, the penultimate one developed about 27 years ago in 1995. In the present case, the hazards associated with the sinkhole included the loss and death of the aquatic flora and fauna, particularly, affecting trout fish cultivation in the area. The overall biological and physical ecosystem came under direct threat and was significantly affected, actively due to the drying of the stream over a stretch of more than > 20 km in downstream areas. The water supply to various sectors including domestic, irrigation, agriculture and horticulture was disrupted and came under threat for future consequences. Field photographs showing the primary and secondary hazards associated with the sinkhole development in the Brengi stream are shown in Fig. 12d–f.

5.5 Future concerns of sinkhole formation

Any hazard interrupting human activity involves a degree of risk, the elements at risk being the life, property and infrastructure (Waltham et al., 2005). The Brengi sinkhole uncovers and represents a characteristic feature of Karst typography in the area. The extensive exposure of Triassic limestone coupled with wet/moist climate shall always render this area vulnerable to such geological processes vis-a-vis development of karst topography leading to geohazards. Moreover, as a result of the current sinkhole, infiltration window and other suitable structural attributes in the area, the development of sinkholes in the future cannot be ruled out. During the field investigation, 5 more relatively smaller sinkholes were identified both upstream and downstream beside the current major sinkhole. Depending

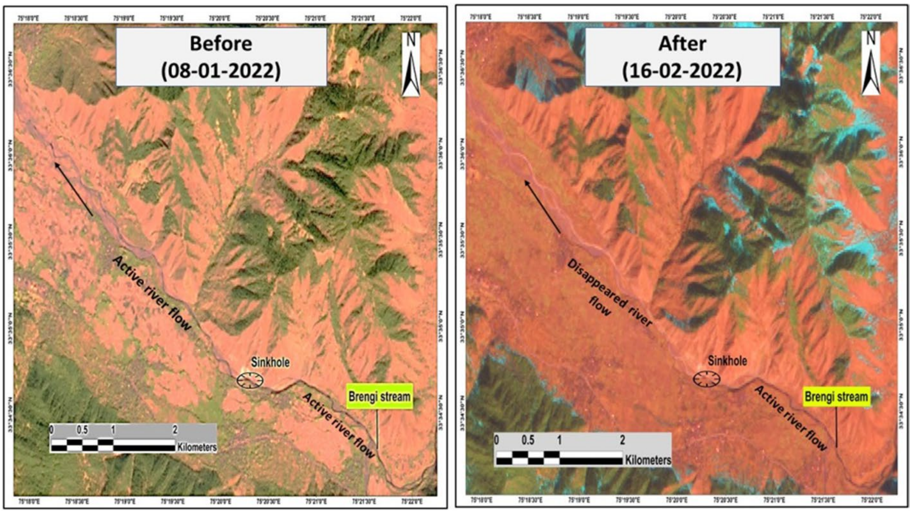

Fig. 11 Sentinnel-2A satellite image showing the pre (08-01-2022)- and post (16-01-2022)-events of sinkhole formation in the Brengi stream. From the image, the complete capture and disappearance of the stream water flow are clearly visible after the development of sinkhole on February 11, 2022

Fig. 12 Field photographs showing **a** newly formed water pool and below it, **b** dry stream bed, **c** measurement of stream flow, **d** masses of dead fishes after sinkhole collapse captured completely stream water, **e** local people catching fishes trapped in small leftover water ponds, **f** dead small fishes and other aquatic creatures near the sinkhole site in the Brengi stream

on the locations, the development of sinkholes may or may not pose risk. However, it is pertinent to note that the development of a sinkhole in the riverbed of Brengi stream posed many risks and affected many sectors heavily dependent on its water flow. As such, the area needs an attention to explore the subsurface characteristics of karsts and its topography. Karst is one of the most vulnerable environments to natural and human-induced hazards. The surface hazards include collapse, subsidence, slope movements and floods, whereas underground hazards include the formation of sinkholes, degraded aquifers and land surface and water pollution.

The development of the current sinkhole significantly affected the irrigation and water supply system in the downstream areas. Many villages relying on the water from the Brengi stream were left dry. In order to understand and elaborate on the influence of water disappearance on the downstream areas, an analysis of the LULC map of the area was carried out. The analysis of LULC from sinkhole to the point where the Brengi stream discharges into the main Jhelum River indicated that a total area of ~ 77.15 km^2 consisting of agricultural land (58%), vegetation (25%), built-up (10%), barren (4%), water (2%), scrub/shrub (1%) and grass (0.1%) comprises major classes. More than 83% of the land use is found heavily dependent on the Brengi stream water supply for domestic and irrigation purposes. Thus, the prolonged drying of the downstream of the Brengi (if any) may disrupt and derail the agricultural-based economy of the area. Any such future event has the potential risk to affect the agro-economy significantly. The map showing the major classes of LULC is shown in Fig. 13. The details are presented in Table 5.

Furthermore, the development of the karst and sinkhole may be associated with a number of future concerns and implications as:

(1) The drying of the downstream areas for longer periods can pose a serious threat to aquatic flora and fauna, thereby disrupting the aquatic ecosystem.
(2) With the drying of the downstream stretch of the river, the seepage is stopped causing an imbalance in the underground water, thereby making the downstream area susceptible to sinkhole formation due to increased effective stress in the subsoil and declining groundwater level.
(3) The discharge going into the sinkhole and not finding outlets immediately might create temporary accumulation and damming of groundwater, which can subsequently lead to underground bursts and the sudden release of the huge quantity of dammed water may therefore cause flash floods.

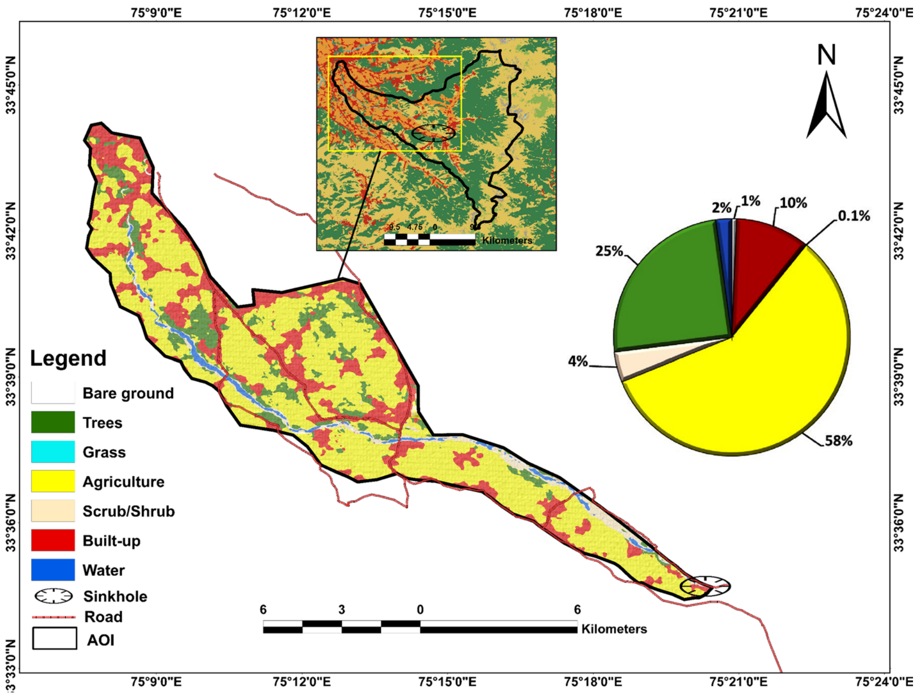

Fig. 13 Map showing the major land-use land-cover (LULC) classes below the location of sinkhole that are susceptible and at a high risk of hazard due to sinkhole formation with a potential to capture the whole stream flow (if any)

Table 5 Area coverage of major classes of LULC or activities below the sinkhole in the study area

S. no.	LULC	Area (km^2)	Accuracy (±)	Percentage (%)
1	Agricultural/ horticulture land	44.66	6.69	58
2	Vegetation	19.25	2.88	25
3	Built-up	7.74	1.11	10
4	Barren ground	3.08	0.46	4
5	Water	1.54	0.23	2
6	Scrub/shrub	0.78	0.11	1
7	Grass	0.096	0.014	0.1

(4) The increased hydrostatic pressures can also lead to hydraulic fracturing of the soft rock causing minor reservoir-induced seismicity in the area.
(5) Increasing demand and pressure on water resources resulting in depletion of ground water tables can further trigger sinkholes to collapse under the pressure of gravity or the void formed by the depleted ground water in the area.
(6) The unexplored and unnoticed sinkholes in the area can be direct and vulnerable possible sources of contamination and pollution of the groundwater under the current scenario of deforestation, urbanization, population growth and ongoing climate change.
(7) Furthermore, the suitable topographic expression of the lithology, subsurface geology and hydro-geochemistry of the area makes it further prone to such responses under the scenario of recent climatic variability (Jeelani, 2008).

6 Conclusion and recommendation

The karst system of Kashmir Himalaya has tremendous and substantial socioeconomic, hydrological and ecological importance as it provides a relatively pristine water supply for drinking, irrigation and other allied purposes. The Brengi stream is a "*Sinking Stream*" wherein the disappearance of flow has been a continuous process through sinkholes developed at many places along its course. The continuous loss of water poses a serious threat to its hydrological and ecological balance, as well as the groundwater and karst springs. On February 11, 2022, a typical "Collapse Sinkhole" formed due to the caving in of the Brengi stream bed at Gratbalpora, Wandevalgam village, near Kokernag located in Kashmir Himalaya.

The sinkhole developed due to the roof rock failure into the existing underlying cave formed within the Triassic limestones of the area. Due to the continuous physical weathering and progressive failure of the steep side walls, the diameter of the sinkhole further expanded on February 26, 2022, resulting in damage to the divergent channel and engulfing the whole stream flow. The present study revealed a major role of prolonged chemical weathering, erosion and structural fabrics in facilitating the slip, collapse and failure of the cap rock of an underlying unknown cavern. The failure was also found to have been aggravated by the heavy overburden alluvial material (basaltic boulders > 60%) and a deep-water column (~ 80 m^3) just present before its actual failure. The present study found the underlying cavern about ~ 100 m long downstream along the run of the stream. There is no way of knowing how many caverns and underground channels exist below the ground surface, but the karst springs indicate that they are very abundant. The sinkhole is a direct indication of the presence of karstification in the area, which, however, is unexplored in detail. Owing to the continuous chemical weathering and denudations of carbonate lithology (Triassic Limestone) under favorable climatic conditions, the existence of a complex underground karst network cannot be ruled out.

The results of the tracer study indicated an anastomosing interconnected array of underground caverns/fractures. The results indicated that the sinkhole has an outlet at Achabal, at a distance of approximately 16 km from the sinkhole. However, this does not rule out the possibility of other outlets in the nearby areas. The other observation wells (Soaf-Shalli, Adigam and Hillar Village) did not show any detectable concentrations of the dye. These results suggest that the water flows in the NW direction from the sinkhole beneath the hillock running parallel to the right bank of the Brengi Stream. The study suggests that the swallowed water by sinkhole on February 11, 2021, should have been also released through these identified outlets. But, the identification of that surplus discharge has either not been witnessed or monitored timely in the area.

Thus, the monitoring of this area by professionals is necessary over the long term to see if any menace signs of sinkhole formation are developing. The key thing in this direction is to be aware of new openings, fracture development and expansion of the current sinkhole. These may act as signs or warnings of imminent collapse. Studies on sinkhole hazard susceptibility, vulnerability and risks are required to be taken up. This step will help to develop better planning and policy strategies for the mitigation of hazards and vulnerable elements in time. Studies are required to develop an underground geological, hydrogeological, or karst framework of the area. Such detailed studies will help the proper management of groundwater resources, karst aquifers and springs and indigenous aquatic life in the area. The present study showed the sinkhole formation at a specific point in time, and this will serve as an important benchmark for future studies.

Supplementary Information The online version contains supplementary material available at https://doi.org/10.1007/s10668-023-03204-1.

Acknowledgements The authors would like to thank the Local People and District Administration for the necessary support during the field work and during the collection of the data. The people involved in this work directly or indirectly are highly acknowledged for their help. The authors are also thankful to the Geological Survey of India for providing Bhukosh data window and United States Geological Survey (USGS) for freely providing the satellite data used in this study.

Authors' contributions Every author has contributed to the successful compilation of this study. RAM, RA, MH and RAD contributed to conceptualization, methodology, writing—original draft, and formal analysis and provided software. STA, GFW, AIA, IAB, MUS and WAB were involved in data curation and formal analysis. RA, GFW and RAM contributed to writing—review and editing. PA, SKB and RAM were involved in review and supervision. All authors read and approved the final manuscript.

Funding No funding was received to carry out this study.

Data availability The data sets that support the results of this study are present within the article.

Declarations

Conflict of interest The authors declare no conflicts of interest.

Ethical approval All the ethical standards of research publishing were taken care of during this study.

References

Ahmed, R., Ahmad, S. T., Wani, G. F., Ahmed, P., Mir, A. A., & Singh, A. (2021). Analysis of landuse and landcover changes in Kashmir valley, India—A review. *GeoJournal*. https://doi.org/10.1007/s10708-021-10465-8

Ahmed, R., Ahmad, S. T., Wani, G. F., Mir, R. A., Almazroui, M., Bansal, J. K., & Ahmed, P. (2022). Glacial lake changes and the identification of potentially dangerous glacial lakes (PDGLs) under warming climate in the Dibang River Basin, Eastern Himalaya, India. *Geocarto International*, 1–27.

Berest, P. (2017). Cases, causes and classifications of craters above salt caverns. *International Journal of Rock Mechanics and Mining Sciences, 100*, 318–329. https://doi.org/10.1016/j.ijrmms.2017.10.025

Bhat, N. A., Jeelani, G., & Ahmad Mir, R. (2021). Application of environmental isotopes and hydrogeochemistry in groundwater management—A case study of Bringi Watershed, Kashmir Himalayas, India. In A. K. Taloor, B. S. Kotlia, & K. Kumar (Eds.), *Water, cryosphere, and climate change in the Himalayas geography of the physical environment.* Springer. https://doi.org/10.1007/978-3-030-67932-3_20

Brinkmann, R., Parise, M., & Dye, D. (2008). Sinkhole distribution in a rapidly developing urban environment: Hillsborough County, Tampa Bay area Florida. *Engineering Geology, 99*(3–4), 169–184.

Coward, J. M. H., Waltham, A. C., & Bowser, R. J. (1972). Karst springs in the Vale of Kashmir. *Journal of Hydrology, 16*(3), 213–223. https://doi.org/10.1016/0022-1694(72)90053-4

E.S.R.I. (2021). https://www.arcgis.com/home/item.html?id=d6642f8a4f6d4685a24ae2dc0c73d4ac

Field, M.S. (2002). A Lexicon of Cave and Karst Terminology with Special reference to Environmental Karst Hydrology, pp. 214. U.S. Environmental Protection Agency, Washington D.C.

Ford, D. C., & Williams, P. (2007). *Karst hydrogeology and geomorphology*. John Wiley and Sons.

G.S.I. (2012). Miscellaneous Publication GSI. No. 30, part X, 30.

Goldscheider, N., Chen, Z., Auler, A. S., Bakalowicz, M., Broda, S., Drew, D., & Veni, G. (2020). Global distribution of carbonate rocks and karst water resources. *Hydrogeology Journal, 28*(5), 1661–1677.

Imdad, K., Rihan, M., Sahana, M., Parween, S., Ahmed, R., Costache, R., Chaudhary, A., & Tripathi, R. (2022). Wetland health, water quality, and resident perceptions of declining ecosystem services: A case study of Mount Abu, Rajasthan, India. Environmental Science and Pollution Research, 1–27, https://doi.org/10.1007/s11356-022-21902-7.

Jeelani, G. (2008). Aquifer response to regional climate variability in a part of Kashmir Himalayas in India. *Hydrogeology Journal, 16*, 1625–1633. https://doi.org/10.1007/s10040-020-02139-5

Jeelani, G., Kumar, U. S., Bhat, N. A., Sharma, S., & Kumar, B. (2015). Variation of δ18O, δD and 3H in karst springs of south Kashmir, western Himalayas (India). *Hydrological Processes, 29*(4), 522–530. https://doi.org/10.1002/hyp.10162

Jeelani, G., Shah, R. A., & Deshpande, R. D. (2018). Assessment of groundwater in karst system of Kashmir Himalayas, India. *Groundwater of South Asia* (pp. 85–100). Springer.

Kuniansky, E. L., Weary, D. J., & Kaufmann, J. E. (2015). The current status of mapping karst areas and availability of public sinkhole-risk resources in karst terrains of the United States. *Hydrogeology Journal, 24*(3), 613–624.

Macleod, R. D., & Congalton, R. G. (1998). A quantitative comparison of change-detection algorithms for monitoring eelgrass from remotely sensed data. *Photogrammetric Engineering and Remote Sensing, 64*(3), 207–216.

Mir, R. A. (2018). Recent changes of two parts of Kolahoi Glacier and its controlling factors in Kashmir basin, western Himalaya. *Remote Sensing Applications: Society and Environment, 11*, 265–281. https://doi.org/10.1016/j.rsase.2018.07.009

Mir, R. A., & Gani, K. M. (2019). Water quality evaluation of the upper stretch of the river Jhelum using multivariate statistical techniques. *Arabian Journal of Geosciences, 12*, 445. https://doi.org/10.1007/s12517-019-4578-7

Mir, R. A., & Jeelani, G. (2015). Hydrogeochemical assessment of River Jhelum and its tributaries for domestic and irrigation purposes, Kashmir valley India. *Current Science, 109*(2), 311–322.

Mir, R. A., Jeelani, G., & Dar, F. A. (2016). Spatio-temporal patterns and factors controlling the hydrogeochemistry of the river Jhelum basin Kashmir Himalaya. *Environmental Monitoring and Assessment, 188*(7), 1–24. https://doi.org/10.1007/s10661-016-5429-6

Mir, R. A., Ahmad, S. A., Akaram, V., & Kumar, V. (2023). Geoheritage and Geotourism Potential of Kalaruch Old Workings (Ancient Mines) and Satbarren (Archeological Stone) in Kashmir Valley of Himalaya. *Geoheritage*, *15*(2), 43.

Parise, M. (2019). Sinkholes. *Encyclopedia of caves* (pp. 934–942). Academic Press.

Payne, S. (2000). Sorption and its effects on transport of organic dyes and cesium in soils. *Organic Geochemistry, 31*, 711–725.

Sahana, M., Dutta, S., & Sajjad, H. (2019). Assessing land transformation and its relation with land surface temperature in Mumbai city, India using geospatial techniques. *International Journal of Urban Sciences, 23*(2), 205–225.
Shah, R. A., & Jeelani, G. (2016). Vulnerability of karst aquifer to contamination: A case study of Liddar catchment, Kashmir Himalayas. *Journal of Himalayan Ecology and Sustainable Development, 11*, 58–72.
Shah, R. A., Jeelani, G., & Goldscheider, N. (2018). Karst geomorphology, cave development and hydrogeology in the Kashmir valley, Western Himalaya, India. *Acta Carsolog*, *47*(1), 1–21.
Sheen, S. W. (2000). A world model of chemical denudation in Karst Terrains. *The Professional Geographer*, *52*(3), 397–406.
Smith, D. I., & Atkinson, T. C. (1972). Process, landform and climate in limestone regions. In E. Derbyshire (Ed.), *Geomorphology and climate* (pp. 367–409). Wiley.
Strzałkowski, P. (2019). Sinkhole formation hazard assessment. *Environmental Earth Sciences, 78*(1), 1–6.
Trillat, M. A. (1899). Sur l'emploi des mati`eres colorantes pour la recherche de l'origine des sources et des eaux d'infiltration. *Comptes Rendus Hebdomadaires Des Séances De L'académie Des Sciences, 128*, 698–702.
Waltham, A. C., M. J. Simms, A. R. Farrant, & H. S. Goldie. (1997) *Karst and caves of Great Britain, geological conservation review series*, 25–98. Chapman and Hall, London.
Waltham, T., Bell, F. G., Culshaw, M. G., Knez, M., & Slabe, T. (2005). *Sinkholes and subsidence: Karst and cavernous rocks in engineering and construction* (Vol. 382). Springer.
White, W. B. (1988). *Geomorphology and hydrology of karst terrains*. Oxford University Press.
Xua, J., Heb, J., & Zhang, L. (2017). Collapse prediction of karst sinkhole via distributed Brillouin optical fiber sensor. *Measurement, 100*, 68–71.

Authors and Affiliations

Riyaz Ahmad Mir[1,2] · Rayees Ahmed[2] · Majid Hussain[3] · Syed Kaiser Bukhari[3] · Pervez Ahmed[2] · Reyaz Ahmad Dar[4] · Syed Towseef Ahmad[2] · Gowhar Farooq Wani[2] · Aasif Ibni Ahad[3] · Abid Farooq Rather[2] · Irshad Ahmad Bhat[2] · Mifta-ul-Shafiq[2] · Waseem Ahmad Bhat[2]

✉ Rayees Ahmed
rayeesrashid84@gmail.com

Riyaz Ahmad Mir
riyazgsi@gmail.com

Majid Hussain
majid.h@nitsri.ac.in

Syed Kaiser Bukhari
kaiserbukhari@nitsri.ac.in

Pervez Ahmed
pervezku@gmail.com

Reyaz Ahmad Dar
reyazsopore@gmail.com

Syed Towseef Ahmad
stawseef77@gmail.com

Gowhar Farooq Wani
gowhernaz@gmail.com

Aasif Ibni Ahad
aasif09phd19@nitsri.ac.in

Abid Farooq Rather
aabidafr@gmail.com

Irshad Ahmad Bhat
irshad.scholar@kashmiruniversity.net

Mifta-ul-Shafiq
saabid9@gmail.com

Waseem Ahmad Bhat
wasimbhat.wb@gmail.com

[1] Geological Survey of India, Srinagar 190008, Jammu and Kashmir, India

[2] Department of Geography and Disaster Management, University of Kashmir, Srinagar 190 006, Jammu and Kashmir, India

[3] Civil Engineering Department, National Institute of Technology, Srinagar 190006, Jammu and Kashmir, India

[4] Department of Earth Sciences, University of Kashmir, Srinagar 190006, Jammu and Kashmir, India